ORIGINAL ARTICLE

Cancer Reports   **WILEY**

Correlations between DW-MRI and ^{18}F-FDG PET/CT parameters in head and neck squamous cell carcinoma following definitive chemo-radiotherapy

Steve Connor[1,2,3] | Cherry Sit[3] | Mustafa Anjari[3] | Teresa Szyszko[4] |
Joel Dunn[4] | Irumee Pai[1,5] | Gary Cook[1,4] | Vicky Goh[1,3]

[1]School of Biomedical Engineering and Imaging Sciences, St Thomas' Hospital, King's College, London, UK

[2]Department of Neuroradiology, King's College Hospital NHS Foundation Trust, London, UK

[3]Department of Radiology, Guy's and St Thomas' NHS Foundation Trust, London, UK

[4]King's College London & Guy's and St. Thomas' PET Centre, London, UK

[5]Department of Otolaryngology, Guy's and St Thomas' NHS Foundation Trust, London, UK

Correspondence
Steve Connor, Neuroradiology Department, Ruskin Wing, Kings College Hospital, Denmark Hill, London SE5 9RS, UK.
Email: steve.connor@kcl.ac.uk

Funding information
Guy's and St Thomas' Charity, Grant/Award Number: EFT130501; Royal College of Radiologists

Abstract

Background: Posttreatment diffusion–weighted magnetic resonance imaging (DW-MRI) and 18F-fluorodeoxygluocose (^{18}F-FDG) positron emission tomography (PET) with computed tomography (PET/CT) have potential prognostic value following chemo-radiotherapy (CRT) for head and neck squamous cell carcinoma (HNSCC). Correlations between these PET/CT (standardized uptake value or SUV) and DW-MRI (apparent diffusion coefficient or ADC) parameters have only been previously explored in the pretreatment setting.

Aim: To evaluate stage III and IV HNSCC at 12-weeks post-CRT for the correlation between SUV_{max} and ADC values and their interval changes from pretreatment imaging.

Methods: Fifty-six patients (45 male, 11 female, mean age 59.9 + − 7.38) with stage 3 and 4 HNSCC patients underwent 12-week posttreatment DW-MRI and ^{18}F-FDG PET/CT studies in this prospective study. There were 41/56 patients in the cohort with human papilloma virus-related oropharyngeal cancer (HPV OPC). DW-MRI (ADC_{max} and ADC_{min}) and ^{18}F-FDG PET/CT (SUV_{max} and SUV_{max} ratio to liver) parameters were measured at the site of primary tumors (n = 48) and the largest lymph nodes (n = 52). Kendall's tau evaluated the correlation between DW-MRI and ^{18}F-FDG PET/CT parameters. Mann-Whitney test compared the post-CRT PET/CT and DW-MRI parameters between those participants with and without 2-year disease-free survival (DFS).

Results: There was no correlation between DW-MRI and ^{18}F-FDG PET/CT parameters on 12-week posttreatment imaging (P = .455-.794; tau = −0.075-0.25) or their interval changes from pretreatment to 12-week posttreatment imaging (P = .1-.946; tau = −0.194-0.044). The primary tumor ADC_{mean} (P = .03) and the interval change in nodal ADC_{min} (P = .05) predicted 2-year DFS but none of the ^{18}F-FDG PET/CT parameters were associated with 2-year DFS.

Conclusions: There is no correlation between the quantitative DWI-MRI and ^{18}F-FDG PET/CT parameters derived from 12-week post-CRT studies. These parameters may be independent biomarkers however in this HPV OPC dominant cohort, only selected ADC parameters demonstrated prognostic significance.

Study was prospectively registered at http://www.controlled-trials.com/ISRCTN58327080

1 | BACKGROUND

Head and neck squamous cell carcinoma (HNSCC) is the seventh most common cancer worldwide.[1] Patients with advanced loco-regional disease can be treated with radiotherapy, or combined chemo-radiotherapy (CRT), but 25% to 50% will have residual disease that requires further intervention.[2,3] Early posttreatment detection of residual tumor is required in order to optimize the outcomes of salvage surgery.[4,5] Unfortunately, clinical assessment and structural imaging are limited in their ability to detect loco-regional residual or recurrent disease due to treatment-related soft tissue distortion.[6-8]

In order to overcome the shortcomings of structural imaging in this clinical scenario, metabolic imaging with 18F-fluorodeoxygluocose (^{18}F-FDG) positron emission tomography (PET) in combination with computed tomography (PET/CT) has become widely utilized.[2,9-12] ^{18}F-FDG PET/CT is reported to be a highly sensitive technique for detection of HNSCC in the post-CRT setting. Semiquantitative analysis of maximum standardized uptake value (SUV_{max}) with ^{18}F-FDG PET-CT has been shown to have prognostic significance, with increased SUV_{max} being associated with treatment failure.[13-18]

Quantitative diffusion-weighted magnetic resonance imaging (DW-MRI) with measurement of the apparent diffusion coefficient (ADC) is another functional imaging technique, which may be used to help distinguish tumor from posttreatment changes and has been applied to the early posttreatment assessment of HNSCC. The majority of studies have found that an increased posttreatment ADC or greater rise in ADC from the pretreatment to the intratreatment or posttreatment studies is a predictor of treatment success.[19-24]

It is still unclear whether ^{18}F-FDG and ADC values provide similar information with regard to viable tumor cells, or whether the two are entirely unrelated biomarkers. Both ADC values and SUV_{max} have shown significant correlation with different histopathological parameters although this may depend on tumor grade.[25-28] There is currently no comparative data on the ability of post-CRT quantitative ^{18}F-FDG PET/CT and DW-MRI to predict post-CRT residual disease, with current evaluations having been limited to comparing these parameters in the pretreatment and intratreatment settings.[29-37] On the one hand, since a post-CRT reduction in SUV_{max} and interval increase in ADC are both markers of treatment success, it would seem logical to expect them to negatively correlate. On the other hand, they reflect different biological processes, so the possibility of independent biomarkers, which are complementary in stratifying the probability of residual disease, should also be explored.

Our hypothesis was that there would be a significant negative linear relationship between ADC and SUV values on 12-week post-CRT studies in patients with stage III and IV HNSCC. Thus, our primary objective was to determine any correlation between ADC and SUV_{max} values on 12-week post-CRT studies, and between their interval changes from pretreatment to 12-week post-CRT studies. Our secondary objective was to evaluate these posttreatment ADC and SUV_{max} values and their interval changes for their ability to predict 2-year DFS outcomes.

2 | METHOD

2.1 | Participants

Participants were recruited for a prospective single center cohort observational study (http://www.controlled-trials.com/ISRCTN58327080) following Research Ethics Committee approval (REC reference 13/LO/1876) and informed consent.

Participants were eligible if: (a) there was a histologically confirmed stage III and IV primary SCC of the head and neck without distant metastatic disease, (b) a 1-cm^2 area of measurable primary tumor and/or nodal tumor on the basis of standard clinico-radiological staging, and (c) curative CRT was planned. Exclusion criteria included prior CRT, an Eastern Cooperative Oncology Group (ECOG) performance status >2, inability to provide informed consent, known allergy to gadolinium-based contrast medium and eGFR<30 mL/min.

2.2 | Treatment and HPV status

Intensity-modulated radiotherapy (IMRT) was delivered as per the standard of care which was 7-Gy in 35 fractions; 2Gy per fraction delivered once daily, 5 days a week. Concomitant intravenous cisplatin at a dose of 35 mg/m^2 every 7 days, starting on day 1 of radiotherapy, was used for all patients with adequate GFR and no contraindications to cisplatin (n = 47) with carboplatin being used if

measured GFR < 50 or if patient had a history of hearing impairment (n = 16). Two patients received radiotherapy alone. HPV status was analyzed for all oropharyngeal and 1/13 other cancers. This involved p16 testing using an immune-stain or high-risk HPV DNA testing using in situ hybridization.

2.3 | Imaging

Participants underwent MRI prior to commencement of CRT, while MRI and ^{18}F-FDG PET/CT were performed at 12 weeks after completion of treatment. Although pretreatment ^{18}F-FDG PET/CT imaging was not mandated as a component of the study, it was performed in selected patients according to the institutional protocol.

2.4 | Magnetic resonance imaging

2.4.1 | Protocol and technique

Participants underwent full standard institutional head and neck soft tissue protocol MRI on a 1.5 Tesla Siemens Magnetom Aera system (Siemen Medical Systems GmbH, Erlangen, Germany) using a surface-phased array neck coil (Table 1). In addition, an echo planar diffusion-weighted sequence was acquired including matched images in the axial plane with multiple b-values (0, 50, 100, 800, and 1500 s/mm^2) and the following scan parameters: repetition time 5900 ms, echo time 60 ms, two signal averages, FOV 240 mm × 240 mm, slice thickness 4 mm with a 0.5 mm slice gap. ADC maps were calculated from the b = 100 and b = 800 values.

2.4.2 | MRI processing and analysis

Processing and analysis of diffusion imaging was performed offline. Data from our institutional Picture Archiving and Communication System (PACS) database were transferred to OsiriX v8.0.2, open-source Mac-based medical image processing software. The regions of interest (ROIs) were placed by a radiologist with 3 years of experience under the supervision of a radiologist with 21 years of experience, who provided training in five cases and ongoing review of a further five cases. Free hand ROIs were placed on the assessable primary tumor and/or largest lymph node using the OsiriX Draw tool with the images magnified to a standard 300%. They were defined on the diffusion-weighted imaging (DWI) b = 800 map as a focus of increased signal relative to background, but with access to the other MRI sequences. Areas of necrosis (non-enhancement and high B0 map signal) and peri-tumoral oedema (avid enhancement and high B0 map signal) were avoided.

ROIs were placed on the baseline and 12-week posttreatment MRI studies in sequence. If there was no longer a 6 mm short axis focus of DWI signal on the posttreatment studies at the location of the initial lesion, a standardized 6 mm diameter circular ROI was placed at its original location by reference to the other sequences and these ROIs were termed "nonmeasurable." All ROIs were then translated directly to a calculated ADC map generated from the b100 and b800 images using the OsiriX ADCmap v1.9 plugin (https://web.stanford.edu/~bah/software/ADCmap/). ADC_{mean} and SD were recorded with ADC_{min} calculated as ADC_{mean} − one SD (rather than absolute ADC_{min}).

2.5 | ^{18}F-FDG PET/CT

2.5.1 | Protocol and technique

The ^{18}F-FDG PET/CT was performed as per institutional clinical practice. Participants were fasted for at least 6 hours prior to administration of 350-400 MBq ^{18}F-FDG. PET/CT scans were acquired 90 minutes after injection from the upper thigh to the base of skull (arms up) with additional local views of the head and neck (arms down) on one of two PET/CT scanners (Siemens mCT Flow VST or GE Discovery DST 710). Images were acquired in 3D time-of-flight (TOF) acquisitions, according to local protocols. A low-dose CT scan (140 kV, 10 mA, 0.5 second rotation time, and 40 mm collimation) was performed at the start in order to provide attenuation correction. Images were reconstructed using ordered subset expectation maximization (OSEM) method. For GE Discovery 710, the parameters were: Algorithm: "VPFX", OSEM, time-of-flight, 2 iterations 24 subsets; Matrix size: 256 × 256 × 47; Pixel Spacing: 2.73 × 2.73 × 3.27; Post-

TABLE 1 MRI protocol

	Plane	Slice thickness/gap	TR/TE	Field of view	Number of averages	Pixel Bandwidth	Flip angle	Acquisition matrix
T1w	Axial	4/0	549/11	220 × 220	1	200	160	384/269
T2w	Axial	4/0	5830/102	220 × 220	1	190	150	384/346
T1w fat saturated-DIXON postgadolinium	Axial	4/0	566/11	220 × 220	1	330	145	320 × 224
STIR	Coronal	3/0.3	3000/35 TI 140	260 × 260	1	220	160	320 × 224
T1w fat sat-DIXON postgadolinium	Coronal	3/0.3	708/10	280 × 280	1	340	145	320 × 320

filter: Gaussian 6.4 mm FWHM. For the Siemens mCT Flow, the parameters were: Algorithm: OSEM, time-of-flight, 2 iterations 21 subsets; Matrix size: $200 \times 200 \times 46$; Pixel Spacing $3.07 \times 4.07 \times 2$; Post-filter: Gaussian 5.0 mm FWHM.

2.5.2 | ^{18}F-FDG PET/CT data processing and analysis

On pretreatment ^{18}F-FDG PET/CT imaging, a 6 mm diameter volume of interest (VOI) was placed at the site of most intense FDG uptake at the site of either the primary lesion and/or the largest lymph node, which was matched to the ROI placed for the MRI analysis. The SUV_{max} was calculated with semiautomated software on a Hermes workstation (Hermes Gold 3, Stockholm). The VOIs were placed by a radiologist with 3 years' experience, under the supervision of a radiologist with 16 years' experience who provided training in five cases and review of further five cases.

The same method for VOI measurement was applied on 12-week posttreatment ^{18}F-FDG PET-CT imaging and SUV_{max} was recorded. The VOIs were chosen with MRI guidance, and always correlated with areas of increased tracer uptake on the pretreatment images. If there was reduced or no uptake on the posttreatment images relative to background, the posttreatment MRI images were referenced and a 6 mm VOI was placed at the same site as the MRI ROI. If necrosis was identified within a lesion, the area of necrosis was excluded as much as possible, and VOI was placed in the area of most intense tracer uptake. Areas of normal physiological uptake were avoided.

A freehand region of interest (ROI) was placed over the right lobe of the liver, at approximately its largest diameter, to record background liver SUV_{max}.[31] This was performed in order to calculate the SUV_{max} ratio to liver parameter.

2.6 | Treatment outcome

Outcome evaluation comprised clinical assessment at 1 year and 2 years following completion of treatment. A 12-week posttreatment positron emission tomography computed tomography (PET CT) study was standard of care and was used to guide clinical management. Treatment failure was determined by cytological or histological confirmation (biopsy or resection) or by serial progression on imaging follow-up. The 2-year DFS was recorded according to status at 2 years following completion of treatment.

2.7 | Statistical analysis

The Shapiro-Wilks normality test determined a proportion of the ADC_{mean} and liver SUV_{max} data to show a significant deviation from normal (with a multiple comparison corrected threshold). Therefore, the primary descriptive statistics focused on the nonparametric

median ± interquartile range) and the primary correlation was performed with the nonparametric Kendall's Tau method.

The correlation between ADC_{mean} and SUV_{max} at the tumor and nodal sites on the 12-week post-CRT studies, and the interval change from pretreatment imaging to 12-week posttreatment studies was analyzed. The threshold for statistical significance was set at $P < .05$. This study provided 95% power to detect a true "moderate" correlation of tau = 0.34 at this threshold.

The same statistical approach was used to extend the comparison to alternative parameters (ADC_{min}, SUV_{max} ratio to liver) on the 12-week posttreatment studies, as well as the interval change from pretreatment imaging to 12-week posttreatment studies. The subgroup of patients with measurable disease as defined by a clear focus of DWI signal on the 12-week posttreatment DW-MRI was also analyzed separately.

Scatter plots of ^{18}F-FDG PET/CT and MRI measures were produced to demonstrate any correlation with 95% confidence intervals.

The Mann-Whitney test was used for a univariate analysis comparing tumor and nodal ADC and SUV_{max} parameters with the dichotomized 2-year DFS.

3 | RESULTS

3.1 | Participants

The participant flowchart is summarized in Figure 1.

There were 70 participants initially enrolled in the study. However, five patients were subsequently withdrawn and a further nine participants did not attend for one of the posttreatment studies (Figure 1). Therefore, 12-week post-CRT ^{18}F-FDG PET-CT and DW-MRI were analyzed for 56 patients (45 male, 11 female, mean age 59.9 + −7.38). Since the ROIs were only placed on 1 cm^2 areas of measurable primary tumor and/or nodal tumor, the measurements were performed at the primary site alone (no measurable pathological lymph nodes, n = 4), the largest lymph node alone (no measurable primary tumor, n = 8) or both sites (n = 44). The tumor site, subsite, and HPV status are documented in Table 2. There was a majority of human papilloma virus-associated oropharyngeal cancer (HPV OPC) participants in this prospectively recruited cohort.

Since pretreatment ^{18}F-FDG PET/CT was performed according to the institutional protocol rather than under the research protocol, it was only available for 43 patients. There were 36/43 patients who also had 12-week post-CRT ^{18}F-FDG PET-CT and DW-MRI available. Therefore, the interval changes from pretreatment to 12-week posttreatment studies could be analyzed in 36 patients with ROIs placed at the largest lymph node alone (n = 6) or both sites (n = 30).

At 2-year follow-up, there were three participants with isolated nodal recurrence, one participant with isolated primary recurrence and two participants with distal metastases alone. The participants with nodal recurrence underwent salvage neck dissection. There were therefore 50/56 patients with 2-year DFS.
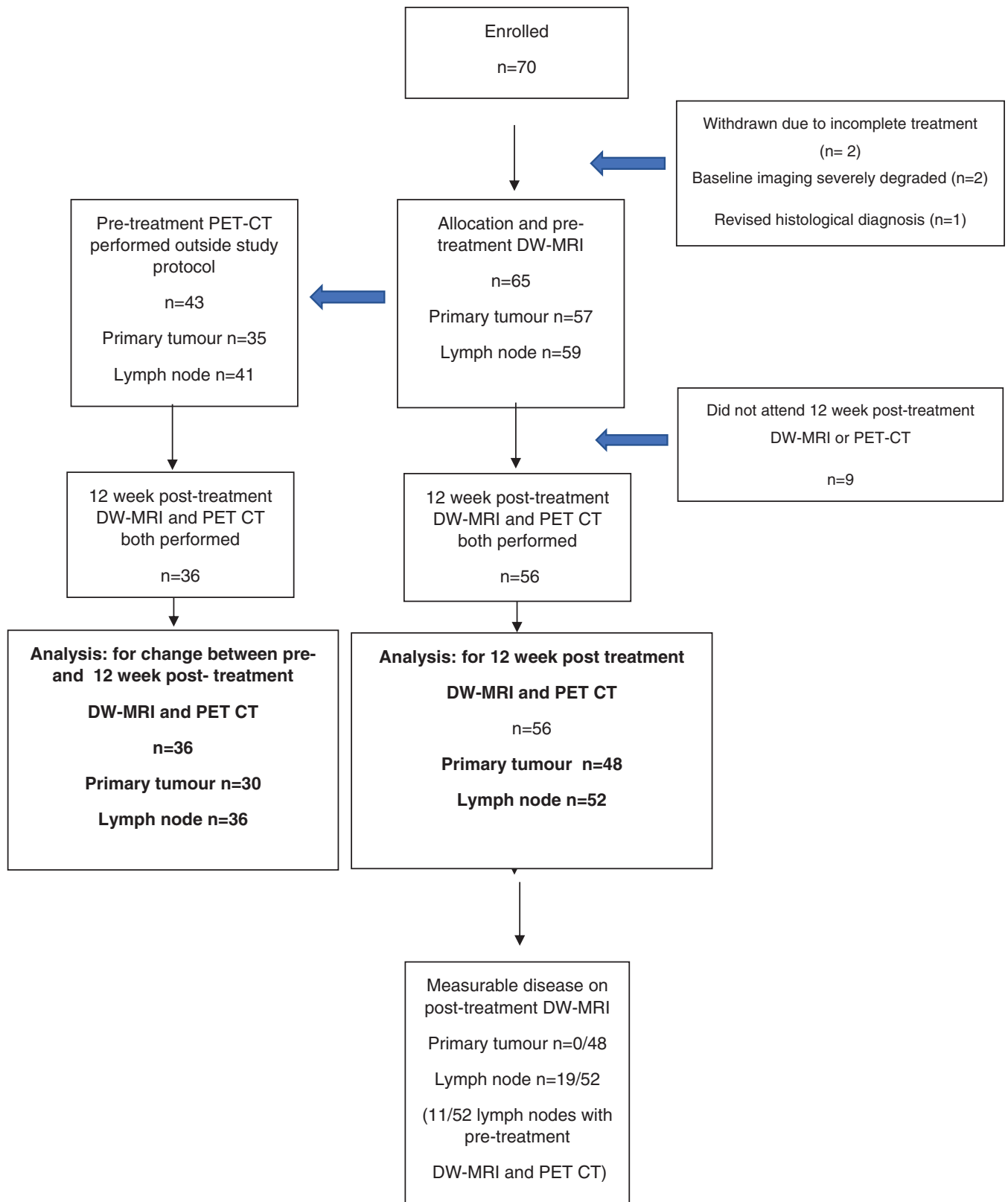
Enrolled

n=70

Withdrawn due to incomplete treatment
(n= 2)

Baseline imaging severely degraded (n=2)

Revised histological diagnosis (n=1)

Pre-treatment PET-CT
performed outside study
protocol

n=43

Primary tumour n=35

Lymph node n=41

Allocation and pre-
treatment DW-MRI

n=65

Primary tumour n=57

Lymph node n=59

Did not attend 12 week post-treatment
DW-MRI or PET-CT

n=9

12 week post-treatment
DW-MRI and PET CT
both performed

n=36

12 week post-treatment
DW-MRI and PET CT
both performed

n=56

**Analysis: for change between pre-
and 12 week post- treatment**

DW-MRI and PET CT

n=36

Primary tumour n=30

Lymph node n=36

Analysis: for 12 week post treatment

DW-MRI and PET CT

n=56

Primary tumour n=48

Lymph node n=52

Measurable disease on
post-treatment DW-MRI

Primary tumour n=0/48

Lymph node n=19/52

(11/52 lymph nodes with
pre-treatment

DW-MRI and PET CT)

FIGURE 1   Participant flow chart

3.1.1 | Associations between post-CRT DW-MRI and PET/CT parameters

The descriptive statistics for the tumor and nodal ADC_{mean}, ADC_{min}, SUV_{max}, SUV_{max} lesion: liver at 12-week posttreatment imaging, together with interval changes from pretreatment imaging are shown in Table 3.

No significant negative correlations were demonstrated between ADC_{mean} and SUV_{max} at the tumor and nodal sites on the 12-week post-CRT studies ($P = .455$-$.794$; tau = -0.075-0.25), or their interval changes from pretreatment to 12-week posttreatment studies ($P = .1$-$.946$; tau = -0.194-0.044). Scatter plots of the correlation are demonstrated in Figure 2. There was also no correlation between any of the other DW-MRI (ADC_{min}) and ^{18}F-FDG PET/CT (SUV_{max} lesion: liver) parameters with respect to the 12-week posttreatment studies or pretreatment to 12-week posttreatment interval changes (Figures 3 and 4). Table 4 demonstrates the correlation of MRI parameters and PET/CT parameters, with Table 5 demonstrating the same correlation but restricted to patients with measurable disease (n = 19/52 lymph nodes) at 12-weeks posttreatment.

3.1.2 | Prediction of 2 year DFS with post-CRT DW-MRI and PET/CT parameters

The comparison of ADC and SUV_{max} parameters in participants with and without 2 year DFS is demonstrated in Table 6. The primary tumor ADC_{mean} at 12-weeks post-CRT DW-MRI ($P = .03$) and the interval change in nodal ADC_{min} from pretreatment to 12-weeks post-CRT DW-MRI ($P = .05$) were associated with 2-year DFS. None of the other ADC parameters and no SUV_{max} parameters were able to predict 2-year DFS.

4 | DISCUSSION

This study provides novel data comparing post-CRT diffusion quantitative DW-MRI and ^{18}F-FDG PET/CT parameters in HNSCC. No

TABLE 2 Patient characteristics of 56 patients (45 male, 11 female, mean age 59.9 + −7.38) patients, indicating site, subsites, and HPV status

Oropharynx	n = 43		
Tongue base	26	HPV +ve	41
Tonsil	16	HPV −ve	2
Soft Palate	1		
Larynx	**n = 8**		
Supraglottic	6	HPV +ve	0
Transglottic	2	HPV −ve	1
		Not tested	7
Hypopharynx	**n = 5**		
Piriform Fossa	5	HPV +ve	0
		HPV −ve	0
		Not tested	5

TABLE 3 Descriptive statistics of ADC_{min} ($\times 10^{-6}$ mm^2/s), ADC_{mean} ($\times 10^{-6}$ mm^2/s), SUV_{max} and SUV_{max}: liver-to-target ratio values for node and tumor, measured at 12-weeks posttreatment, and absolute interval change between pretreatment and 12-weeks posttreatment values

	n	Mean	SD	LQ	Median	UQ
Node ADC_{min} at 12 weeks	52	1028.70	245.04	888.25	1030.00	1163.73
Tumor ADC_{min} at 12 weeks	48	1373.79	282.27	1181.00	1369.46	1583.78
Change in node ADC_{min} pre-12 weeks	52	338.07	343.62	159.75	337.00	470.71
Change in tumor ADC_{min} pre-12 weeks	48	732.17	333.37	461.62	780.00	971.00
Node ADC_{mean} at 12 weeks	52	1462.88	250.71	1326.14	1458.28	1573.10
Tumor ADC_{mean} at 12 weeks	48	1830.08	270.47	1614.87	1821.60	1984.39
Change in node ADC_{mean} pre-12 weeks	52	520.74	322.15	261.54	513.90	713.33
Change in tumor ADC_{mean} pre-12 weeks	48	926.01	294.51	745.32	921.63	1089.01
	n	Mean	SD	LQ	Median	UQ
Node SUV_{max} at 12 weeks	52	1.89	0.55	1.52	1.83	2.33
Tumor SUV_{max} at 12 weeks	48	3.00	0.88	2.32	2.96	3.62
Change in node SUV_{max} pre-12 weeks	36	−7.11	4.43	−9.95	−6.39	−4.25
Change in tumor SUV_{max} pre-12 weeks	30	−10.24	6.78	−13.73	−10.31	−5.15
Liver: node SUV_{max} at 12 weeks	52	0.72	0.20	0.56	0.71	0.88
Liver: tumor SUV_{max} at 12 weeks	48	1.17	0.35	0.91	1.09	1.36
Change in liver: node SUV_{max} pre-12 weeks	36	−2.57	1.75	−3.58	−2.33	−1.75
Change in liver: tumor SUV_{max} pre-12 weeks	30	−3.74	2.67	−5.01	−3.48	−1.65

Abbreviations: LQ, lower quartiles; UQ, upper quartiles.

FIGURE 2 Scatter plots of SUV$_{max}$ vs ADC$_{mean}$ at 12-weeks post CRT for (A) primary tumor and (B) lymph node as well as scatter plots for changes in SUV$_{max}$ vs changes in ADC$_{mean}$ from pretreatment to 12-week posttreatment for (C) primary tumor and (D) lymph node. PET measures (y-axes) and MRI measures (x-axes). Line of best fit (blue) with 95% confidence intervals shown overlaid (grey)
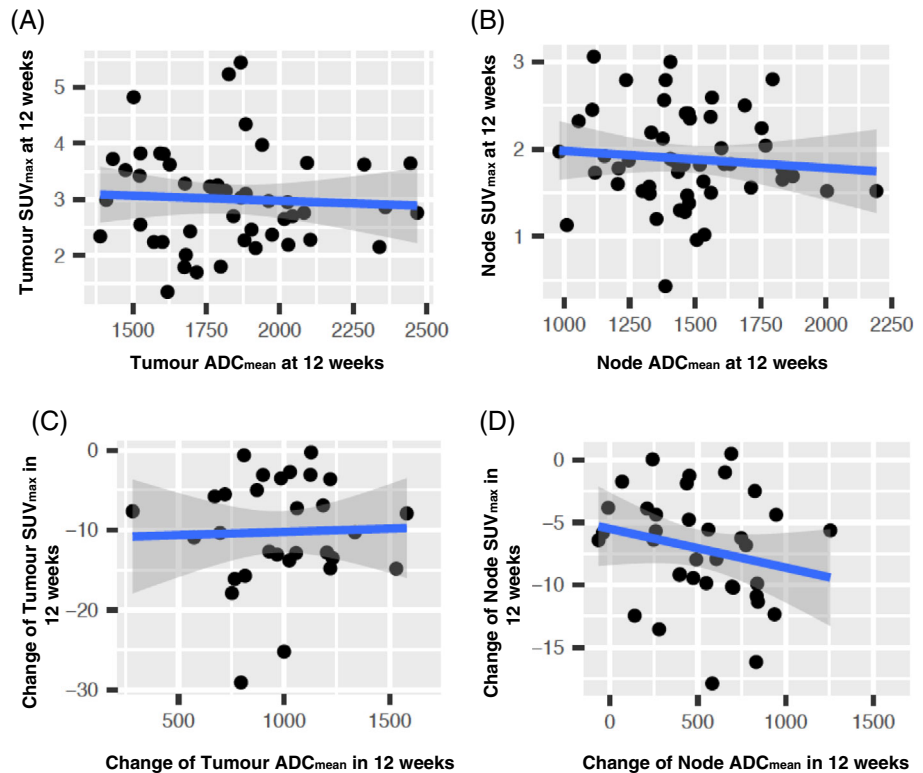
correlation was demonstrated between ADC$_{mean}$ and SUV$_{max}$ on 12-week post-CRT studies, or between the interval change in ADC$_{mean}$ and SUV$_{max}$ values from pretreatment to 12-week post-CRT studies in this HPV OPC dominant cohort with stage III and IV HNSCC. There was also no relationship when comparisons were extended to alternative posttreatment ^{18}F-FDG PET and MRI parameters (ADC$_{min}$, SUV$_{max}$ ratio of tumor to liver) or when only participants with measurable disease on posttreatment DW-MRI studies were analyzed. Only the 12-week post-CRT primary tumor ADC$_{mean}$ and interval change between pretreatment and 12-week post-CRT nodal ADC$_{min}$ were predictive of 2 year DFS.

^{18}F-FDG PET/CT and DW-MRI play an increasing role in the management of high stage HNSCC, and have both been used to provide prognostic biomarkers following CRT treatment. SUV indicates tumor metabolism and ADC reflects microscopic features such as tumor cellularity. ADC may also represent a surrogate marker for hypoxia as indicated by ^{18}F-FMISO PET/CT.[37] While some studies have focused on the role of pretreatment SUV$_{max}$[35,34,38-45] and ADC in assisting the early prediction of treatment failure,[6,20,21,23,34,36-50] a posttreatment assessment of SUV$_{max}$ and ADC values has proved most useful to date and was the focus of this study.

Posttreatment ^{18}F-FDG PET/CT is an established technique for the evaluation of post-CRT advanced HNSCC.[2,9-12] Since treatment-induced inflammation in the very early posttreatment period may lead to false positive studies,[16] ^{18}F-FDG PET/CT is usually delayed until 12 weeks following the completion of CRT in order to increase the specificity.[2,17,18] Semiquantitative analysis demonstrating increased posttreatment SUV$_{max}$ values and lack of significant reduction in SUV$_{max}$ values within loco-regional tumor has been shown to indicate treatment failure.[13-18,29,33] Similarly, quantitative DW-MRI has been investigated in the posttreatment setting, with a higher ADC, or a greater interval increase from pre- to intra- or posttreatment ADC,[19-24] being associated with loco-regional treatment success.

It would therefore be useful to establish whether the posttreatment DW-MRI and ^{18}F-FDG PET/CT-based parameters are correlated with each other. While treatment failure is associated with interval changes in both posttreatment SUV$_{max}$ and ADC, they may still have a complementary role in evaluating treatment response if they are demonstrated to be independent variables.[34,35] This would inform on appropriate early posttreatment protocols and the applicability of new technologies such as PET-MRI, which would measure both parameters simultaneously.

Previous reports comparing SUV and ADC parameters in HNSCC are restricted to the pretreatment scenario and these have demonstrated disparate results. Choi et al (n = 31)[30] and Nakajo et al (n = 26)[34] reported significant negative correlations between pretreatment ADC and SUV. It was argued that the glycolytic activity evaluated with ^{18}F-FDG PET-CT is therefore significantly related with the microstructural environment evaluated by DW-MRI in patients with HNSCC. In contrast, Varoqaux et al (n = 33)[36] and Freuhwald-Wallamar et al (n = 46)[31] showed no statistical relationship, and hence identified pretreatment SUV and ADC as potentially independent biomarkers in HNSCC. One study has compared quantitative DW-MRI and ^{18}F-FDG PET/CT parameters in the posttreatment setting at another tumor site, with ADC$_{min}$ and SUV$_{max}$ found not to be significantly correlated in recurrent cervical (gynecological) cancer.[51]

Alternative ^{18}F-FDG PET/CT and ADC parameters were also evaluated. First, although SUV is the more commonly used parameter
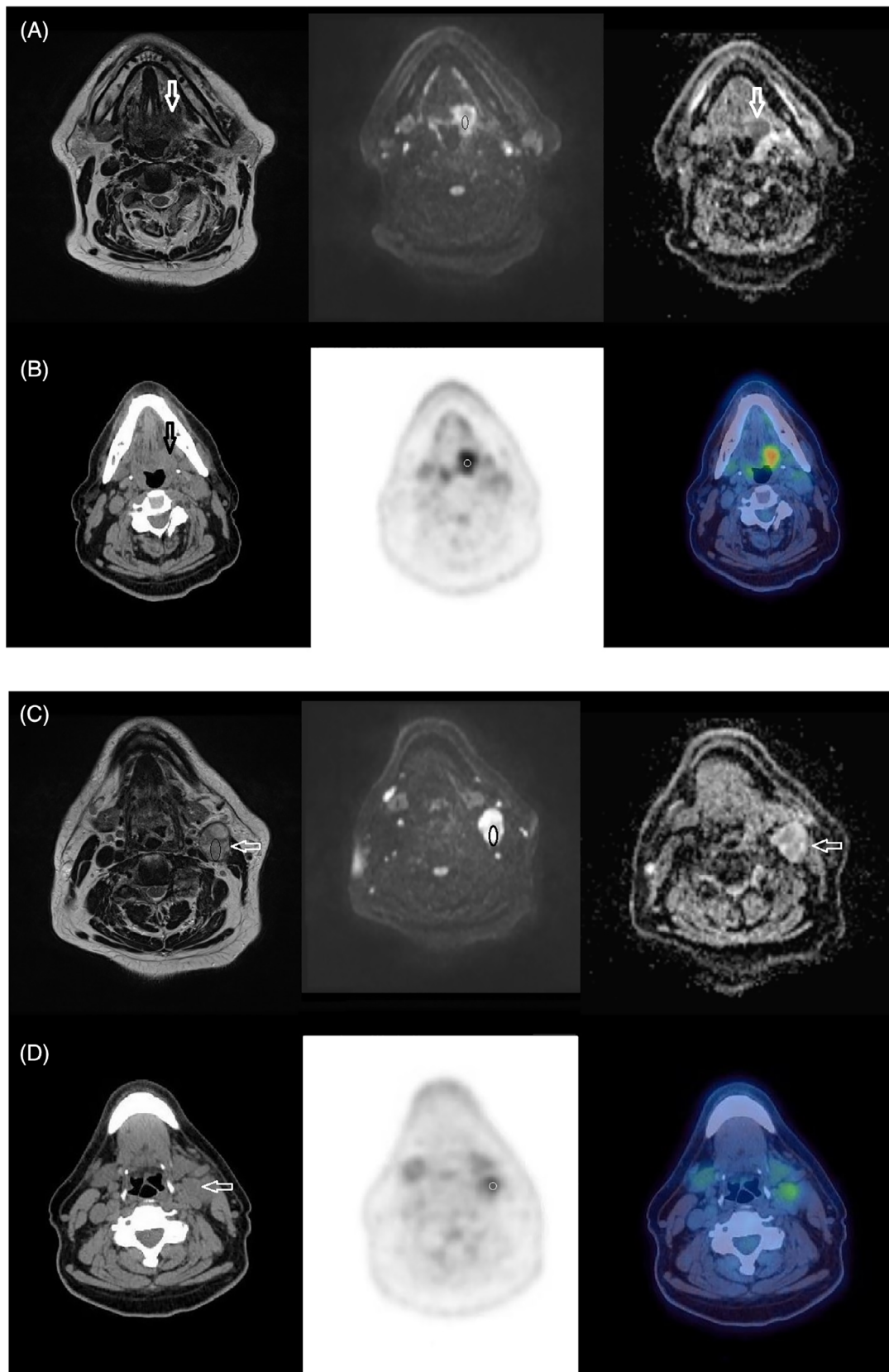
FIGURE 3 Pretreatment MRI and FDG PET/CT study in a 64-year-old male patient with T2N2b left oropharynx tumor. T2W, b = 800 DWI and ADC map (b = 100-800) MRI images (A and C) and CT, PET, PET/CT fused images (B and D) indicating the left glosso-tonsillar sulcus tumor (arrows in A and B) and left level 2 lymph node (arrows in C and D). The ROIs on the MRI study include areas of increased DWI signal corresponding to intermediate T2w signal in the cores of the primary and nodal tumor as indicated (ovals in A and C). The 6 mm VOI on the PET-CT study is seen within the central portion of the primary and nodal tumor (circles in B and D)
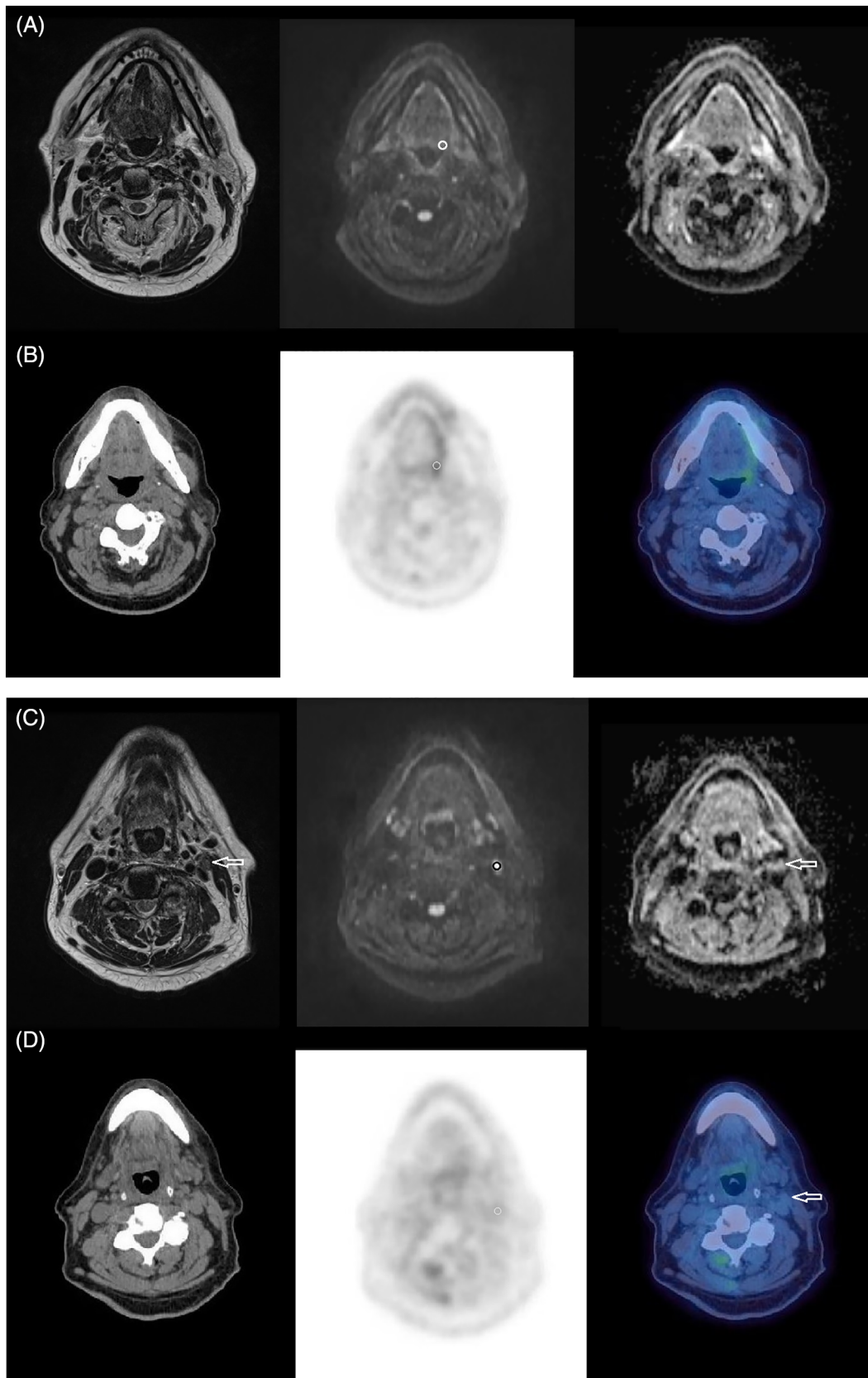
FIGURE 4 12-week post-chemo-radiotherapy MRI and PET/CT study in the same patient. T2w, b = 800 DWI and ADC map (b = 100-800) MRI images (A and C) and CT, PET, PET/CT fused image (B and D) indicating the site of the previous left glosso-tonsillar sulcus tumor, which is now nonmeasurable and left level 2 lymph node, which has markedly reduced in size (arrows in C and D). The 6 mm ROIs on the MRI study are placed at the site of the previous primary tumor (circle in A) and at the residual nodal tumor as indicated (circle in B). The corresponding 6 mm VOI on the PET-CT study is seen within the central portion of the primary and nodal tumor (circles in B and D)

TABLE 4 Correlation of MRI-DWI parameters (ADC$_{min}$ and ADC$_{mean}$) against PET parameters (SUV$_{max}$, SUV$_{max}$: liver-to-target ratio) at 12 weeks, and absolute interval change between pretreatment and 12 weeks posttreatment values

MRI (X)	PET (Y)	n	tau	*P*-value
Node ADC$_{mean}$ at 12 weeks	Node SUV$_{max}$ at 12 weeks	52	−0.061	.528
Node ADC$_{min}$ at 12 weeks	Node SUV$_{max}$ at 12 weeks	52	−0.025	.794
Tumor ADC$_{mean}$ at 12 weeks	Tumor SUV$_{max}$ at 12 weeks	48	−0.075	.455
Tumor ADC$_{min}$ at 12 weeks	Tumor SUV$_{max}$ at 12 weeks	48	−0.042	.676
Node ADC$_{mean}$ at 12 weeks	SUV$_{max}$ liver: node at 12 weeks	52	−0.027	.776
Node ADC$_{min}$ at 12 weeks	SUV$_{max}$ liver: node at 12 weeks	52	−0.034	.723
Tumor ADC$_{mean}$ at 12 weeks	SUV$_{max}$ liver: tumor at 12 weeks	48	−0.048	.639
Tumor ADC$_{min}$ at 12 weeks	SUV$_{max}$ liver: tumor at 12 weeks	48	−0.059	.551
Node ADC$_{mean}$ change pre-12 weeks	Node SUV$_{max}$ change pre-12 weeks	36	−0.194	.100
Node ADC$_{min}$ change pre-12 weeks	Node SUV$_{max}$ change pre-12 weeks	36	−0.101	.946
Tumor ADC$_{mean}$ change pre-12 weeks	Tumor SUV$_{max}$ change pre-12 weeks	30	0.030	.832
Tumor ADC$_{min}$ change pre-12 weeks	Tumor SUV$_{max}$ change pre-12 weeks	30	0.039	.762
Node ADC$_{mean}$ change pre-12 weeks	SUV$_{max}$ liver: node change pre-12 weeks	36	−0.175	.138
Node ADC$_{min}$ change pre-12 weeks	SUV$_{max}$ liver: node change pre-12 weeks	36	0.022	.860
Tumor ADC$_{mean}$ change pre-12 weeks	SUV$_{max}$ liver: tumor pre-12 weeks	30	0.025	.860
Tumor ADC$_{min}$ change pre-12 weeks	SUV$_{max}$ liver: tumor change pre-12 weeks	30	0.044	.735

TABLE 5 Correlation of MRI-DWI parameters (ADC$_{min}$ and ADC$_{mean}$) against PET parameters (SUV$_{max}$, SUV$_{max}$ liver-to-target ratio) in patients with measurable nodal disease at 12 weeks, and absolute interval change between pretreatment and 12-weeks post treatment values

MRI (X)	PET (Y)	n	tau	*P*-value
Node ADC$_{mean}$ at 12 weeks	Node SUV$_{max}$ at 12 weeks	19	−0.035	.834
Node ADC$_{min}$ at 12 weeks	Node SUV$_{max}$ at 12 weeks	19	−0.199	.234
Node ADC$_{mean}$ at 12 weeks	SUV$_{max}$ liver: node at 12 weeks	19	0.006	1.000
Node ADC$_{min}$ at 12 weeks	SUV$_{max}$ liver: node at 12 weeks	19	−0.158	.368
Node ADC$_{mean}$ change pre-12 weeks	Node SUV$_{max}$ change pre-12 weeks	11	−0.236	.359
Node ADC$_{min}$ change pre-12 weeks	Node SUV$_{max}$ change pre-12 weeks	11	−0.055	.879
Node ADC$_{mean}$ change pre-12 weeks	SUV$_{max}$ liver: node change pre-12 weeks	11	−0.236	.359
Node ADC$_{min}$ change pre-12 weeks	SUV$_{max}$ liver: node change pre-12 weeks	11	−0.055	.879

in the assessment of HNSCC treatment response,[13-18] the role of absolute SUV values in the posttreatment evaluation of HNSCC with ^{18}F-FDG PET/CT has been questioned.[10,52] As an alternative, ^{18}F-FDG uptake may be measured relative to normal tissue/background tissue, and quantitative interpretative criteria such as the Porceddu, Hopkins, and Deauville scoring systems are based on this approach.[53-55] Zhong et al evaluated these scoring systems and found that they demonstrated high specificity, PPV, and NPV.[56] Tumor uptake exceeding liver tracer uptake is indicative of disease in all these criteria, and hence we decided to include tumor SUV to liver ratio as another ^{18}F-FDG PET/CT parameter. Some previous studies have demonstrated total lesional glycolysis (TLG) to be a superior predictor of HNSCC treatment outcomes[57]; however, this requires an assessment of metabolic tumor volume, which was not possible in many of the posttreatment cases, where there was no definable FDG uptake and a standardized small VOI was placed. Second, with respect

to the DW-MRI parameters, both ADC$_{mean}$ and ADC$_{min}$ were evaluated in this study since each has previously been applied to previous comparisons of quantitative DW-MRI with ^{18}F-FDG PET/CT on pretreatment imaging.[35,36]

It is of note that while selected ADC parameters were able to predict treatment outcomes in this study, none of the SUV$_{max}$ parameters proved prognostically useful in this study. Some previous studies have shown that posttreatment SUV$_{max}$ is a less accurate predictor of outcome in HPV OPC cohorts.[58,59] In addition, the unexpectedly high rate of HPV-OPC participant recruitment also resulted in low rate of treatment failure such that it was suboptimally powered for the comparison of quantitative DW-MRI and ^{18}F-FDG PET/CT parameters with 2-year DFS.

There are potential shortcomings with the study methodology. First, there are greater challenges with the accurate placement and measurement of ADC and SUV in the posttreatment setting. For

TABLE 6 Two-year disease-free survival and comparison of ADC and SUV_{max} parameters in participants with and without 2-year disease-free survival

Parameter	Total no. participants	No 2 year DFS (no. participants)	2 year DFS (no. participants)	P value (parameter when no 2 year DFS vs 2 year DFS)
Node ADC_{min} at 12 weeks	52	6	46	.06
Tumor ADC_{min} at 12 weeks	48	6	42	.89
Change in node ADC_{min} pre-12 weeks	52	6	46	.05
Change in tumor ADC_{min} pre-12 weeks	48	5	43	.75
Node ADC_{mean} at 12 weeks	52	6	46	.08
Tumor ADC_{mean} at 12 weeks	48	6	42	.03
Change in node ADC_{mean} pre-12 weeks	52	6	46	.10
Change in tumor ADC_{mean} pre-12 weeks	48	5	43	.88
Parameter	Total no. participants	No 2 year DFS (no. participants)	2 year DFS (no. participants)	P value (parameter when no 2 year DFS vs 2 year DFS)
Node SUV_{max} at 12 weeks	52	6	46	.48
Tumor SUV_{max} at 12 weeks	48	6	42	.21
Change in node SUV_{max} pre-12 weeks	36	3	33	.92
Change in tumor SUV_{max} pre-12 weeks	30	2	28	.86
Liver: node SUV_{max} at 12 weeks	52	6	46	.27
Liver: tumor at 12 weeks	48	6	42	.40
Change in liver: node SUV_{max} pre-12 weeks	36	3	33	.82
Change in liver: tumor SUV_{max} pre-12 weeks	30	2	28	.57

instance, there is a reduction in conspicuity of any anatomical tumor target on MRI and the qualitative assessment of the tumor site may not detect FDG tracer greater than background on ^{18}F-FDG PET/CT. This resulted in there being only one third of nodal sites and no primary tumor sites which demonstrated a clear DWI focus to guide the ROI placement on the 12-week posttreatment DW-MRI studies. In addition, the DW-MRI and 18F-PET-CT measurements should ideally have been colocalized, but no fusion of the MRI and 18F-PET/CT data sets was feasible. Second, we do not present inter-observer agreement statistics as part of this study and this would be particularly pertinent to the posttreatment analysis. Varoquaz et al[36] has previously evaluated reproducibility of pretreatment ADC and SUV measurements with ICC > 0.9 for both. Third, the HPV-OPC dominant cohort is a potential confounding factor in this study with its unique histopathological characteristics[60] and differing tumor metabolism.[61] It is recognized that pretreatment ADC values are lower and over a wider range in HPV OPC,[62,63] which may influence posttreatment ADC values or their interval change.

5 | CONCLUSION

We provide the first direct comparison of posttreatment DW-MRI and ^{18}F-FDG PET/CT variables and their interval change from pretreatment values in patients with stage III and IV HNSCC. There was no significant negative linear relationship between ADC and SUV values on 12-week post-CRT studies or their interval changes in this HPV OPC dominant cohort. None of the SUV_{max} parameters and only

selected ADC parameters were associated with 2-year disease-free outcome. Since both the relationship between ADC and SUV values and the prognosis is influenced by HPV OPC status, further studies should focus on HPV negative HNSCC to determine whether DW-MRI and ^{18}F-FDG PET/CT provide independent biomarkers in the post-CRT setting.

AUTHOR CONTRIBUTIONS

All authors had full access to the data in the study and take responsibility for the integrity of the data and the accuracy of the data analysis. *Conceptualization*, SC, VG; *Methodology*, SC, VG, GC, TS; *Investigation*, SC, CS, MA; *Formal Analysis*, SC, JD; *Data Curation*, MA, SC; *Writing—Original Draft*, SC; *Writing—Review & Editing*, SC, VG, GC, TS, IP; *Visualization*, JD, SC, CS; *Supervision*, SC, VG; *Project Administration*, SC; *Funding Acquisition*, SC.

CONFLICT OF INTEREST

The authors have stated explicitly that there are no conflicts of interest in connection with this article.

DATA AVAILABILITY STATEMENT

The data that support the findings of this study are available from the corresponding author upon reasonable request.

ETHICAL STATEMENT

Institutional approval from the Research Ethics Committee (REC reference 13/LO/1876) and informed consent were obtained from all participants. The study conforms to recognized standards of the Declaration of Helsinki.

ORCID

Steve Connor https://orcid.org/0000-0001-5502-4972

REFERENCES

1. Ferlay J, Colombet M, Soerjomataram I, et al. Estimating the global cancer incidence and mortality in 2018: GLOBOCAN sources and methods. *Int J Cancer*. 2019;144:1941-1953.
2. Ul-Hassan F, Simo R, Guerrero-Urbano T, Oakley R, Jeannon JP, Cook GJ. Can (18)F-FDG PET/CT reliably assess response to primary treatment of head and neck cancer? *Clin Nucl Med*. 2013;38:263-265.
3. Eisbruch A, Schwartz M, Rasch C, Vineberg K, Damen E, Van As CJ, Marsh R, Pameijer FA and Balm AJ. Dysphagia and aspiration after chemoradiotherapy for head-and-neck cancer: which anatomic structures are affected and can they be spared by IMRT? *Int J Radiat Oncol Biol Phys* 2004; 60: 1425–1439.
4. Kim AJ, Suh JD, Sercarz JA, et al. Salvage surgery with free flap reconstruction: factors affecting outcome after treatment of recurrent head and neck squamous carcinoma. *Laryngoscope*. 2007;117:1019-1023.
5. Agra IM, Carvalho AL, Ulbrich FS, et al. Prognostic factors in salvage surgery for recurrent oral and oropharyngeal cancer. *Head Neck*. 2006;28:107-113.
6. King AD, Chow KK, Yu KH, et al. Head and neck squamous cell carcinoma: diagnostic performance of diffusion-weighted MR imaging for the prediction of treatment response. *Radiology*. 2013;266:531-538.
7. Hermans R, Pameijer FA, Mancuso AA, Parsons JT, Mendenhall WM. Laryngeal or hypopharyngeal squamous cell carcinoma: can follow-up CT after definitive radiation therapy be used to detect local failure earlier than clinical examination alone? *Radiology*. 2000;214:683-687.
8. Zbaren P, Triantafyllou A, Devaney KO, et al. Preoperative diagnostic of parotid gland neoplasms: fine-needle aspiration cytology or core needle biopsy? *Eur Arch Otorhinolaryngol*. 2018;275:2609-2613.
9. Mehanna H, Wong WL, McConkey CC, et al. PET-CT surveillance versus neck dissection in advanced Head and neck cancer. *N Engl J Med*. 2016;374:1444-1454.
10. Ong SC, Schoder H, Lee NY, et al. Clinical utility of 18F-FDG PET/CT in assessing the neck after concurrent chemoradiotherapy for Locoregional advanced head and neck cancer. *J Nucl Med*. 2008;49:532-540.
11. Kao J, Vu HL, Genden EM, et al. The diagnostic and prognostic utility of positron emission tomography/computed tomography-based follow-up after radiotherapy for head and neck cancer. *Cancer*. 2009;115:4586-4594.
12. Martin RC, Fulham M, Shannon KF, et al. Accuracy of positron emission tomography in the evaluation of patients treated with chemoradiotherapy for mucosal head and neck cancer. *Head Neck*. 2009;31:244-250.
13. Castelli J, De Bari B, Depeursinge A, et al. Overview of the predictive value of quantitative 18 FDG PET in head and neck cancer treated with chemoradiotherapy. *Crit Rev Oncol Hematol*. 2016;108:40-51.
14. Chan JYK, Sanguineti G, Richmon JD, Marur S. Retrospective review of positron emission tomography with contrast-enhanced computed tomography in the posttreatment setting in human papillomavirus–associated oropharyngeal carcinoma. *Arch Otolaryngol Head Neck Surg*. 2012;138:1040-1046.
15. Kim R, Ock C-Y, Keam B, et al. Predictive and prognostic value of PET/CT imaging post-chemoradiotherapy and clinical decision-making consequences in locally advanced head & neck squamous cell carcinoma: a retrospective study. *BMC Cancer*. 2016;16:116.
16. Matoba M, Tuji H, Shimode Y, Kondo T, Oota K, Tonami H. The role of changes in maximum standardized uptake value of FDG PET-CT for posttreatment surveillance in patients with head and neck squamous cell carcinoma treated with chemoradiotherapy: preliminary findings. *Br J Radiol*. 2017;90:20150404.
17. Moeller BJ, Rana V, Cannon BA, et al. Prospective risk-adjusted [18F] fluorodeoxyglucose positron emission tomography and computed tomography assessment of radiation response in head and neck cancer. *J Clin Oncol*. 2009;27:2509-2515.
18. Sherriff JM, Ogunremi B, Colley S, Sanghera P, Hartley A. The role of positron emission tomography/CT imaging in head and neck cancer patients after radical chemoradiotherapy. *Br J Radiol*. 2012;85:e1120-e1126.
19. Berrak S, Chawla S, Kim S, et al. Diffusion weighted imaging in predicting progression free survival in patients with squamous cell carcinomas of the head and neck treated with induction chemotherapy. *Acad Radiol*. 2011;18:1225-1232.
20. Matoba M, Tuji H, Shimode Y, et al. Fractional change in apparent diffusion coefficient as an imaging biomarker for predicting treatment response in head and neck cancer treated with chemoradiotherapy. *AJNR Am J Neuroradiol*. 2014;35:379-385.
21. Marzi S, Piludu F, Sanguineti G, et al. The prediction of the treatment response of cervical nodes using intravoxel incoherent motion diffusion-weighted imaging. *Eur J Radiol*. 2017;92:93-102.
22. Schouten CS, de Bree R, van der Putten L, et al. Diffusion-weighted EPI- and HASTE-MRI and 18F-FDG-PET-CT early during chemoradiotherapy in advanced head and neck cancer. *Quant Imaging Med Surg*. 2014;4:239-250.
23. King AD, Mo FK, Yu KH, et al. Squamous cell carcinoma of the head and neck: diffusion-weighted MR imaging for prediction and monitoring of treatment response. *Eur Radiol*. 2010;20:2213-2220.
24. Vandecaveye V, Dirix P, De Keyzer F, et al. Diffusion-weighted magnetic resonance imaging early after chemoradiotherapy to monitor treatment response in head-and-neck squamous cell carcinoma. *Int J Radiat Oncol Biol Phys*. 2012;82:1098-1107.
25. Rasmussen JH, Olin A, Lelkaitis G, et al. Does multiparametric imaging with ^{18}F-FDG-PET/MRI capture spatial variation in immunohistochemical cancer biomarkers in head and neck squamous cell carcinoma? *Br J Cancer*. 2020;123:46-53.
26. Surov A, Stumpp P, Meyer HJ, et al. Simultaneous (18)F-FDG-PET/MRI: associations between diffusion, glucose metabolism and histopathological parameters in patients with head and neck squamous cell carcinoma. *Oral Oncol*. 2016;58:14-20.
27. Surov A, Meyer HJ, Höhn AK, Winter K, Sabri O, Purz S. Associations between [18F]FDG-PET and complex histopathological parameters including tumor cell count and expression of KI 67, EGFR, VEGF, HIF-1α, and p53 in head and neck squamous cell carcinoma. *Mol Imaging Biol*. 2019;21:368-374.
28. Yokobori Y, Toyoda M, Sakakura K, Kaira K, Tsushima Y, Chikamatsu K. (18)F-FDG uptake on PET correlates with biological potential in early oral squamous cell carcinoma. *Acta Otolaryngol*. 2015;135:494-499.
29. Becker M, Varoquaux AD, Combescure C, et al. Local recurrence of squamous cell carcinoma of the head and neck after radio(chemo) therapy: diagnostic performance of FDG-PET/MRI with diffusion-weighted sequences. *Eur Radiol*. 2018;28:651-663.
30. Choi SH, Paeng JC, Sohn CH, et al. Correlation of 18F-FDG uptake with apparent diffusion coefficient ratio measured on standard and

high b value diffusion MRI in head and neck cancer. *J Nucl Med*. 2011;52:1056-1062.

31. Fruehwald-Pallamar J, Czerny C, Mayerhoefer ME, et al. Functional imaging in head and neck squamous cell carcinoma: correlation of PET/CT and diffusion-weighted imaging at 3 Tesla. *Eur J Nucl Med Mol Imaging*. 2011;38:1009-1019.

32. Leifels L, Purz S, Stumm P, et al. Associations between ^{18}F-FDG-PET, DWI, and DCE parameters in patients with Head and neck squamous cell carcinoma depend on tumor grading. *Contrast Media Mol Imaging*. 2017;2017:5369625.

33. Martins EB, Chojniak R, Kowalski LP, Nicolau UR, Lima EN, Bitencourt AG. Diffusion-weighted MRI in the assessment of early treatment response in patients with squamous-cell carcinoma of the head and neck: comparison with morphological and PET/CT findings. *PLoS One*. 2015;10:e0140009.

34. Nakajo M, Nakajo M, Kajiya Y, et al. FDG PET/CT and diffusion-weighted imaging of head and neck squamous cell carcinoma: comparison of prognostic significance between primary tumor standardized uptake value and apparent diffusion coefficient. *Clin Nucl Med*. 2012;37:475-480.

35. Preda L, Conte G, Bonello L, et al. Combining standardized uptake value of FDG-PET and apparent diffusion coefficient of DW-MRI improves risk stratification in head and neck squamous cell carcinoma. *Eur Radiol*. 2016;26:4432-4441.

36. Varoquaux A, Rager O, Lovblad KO, et al. Functional imaging of head and neck squamous cell carcinoma with diffusion-weighted MRI and FDG PET/CT: quantitative analysis of ADC and SUV. *Eur J Nucl Med Mol Imaging*. 2013;40:842-852.

37. Wiedenmann N, Grosu A-L, Buchert M. The utility of multiparametric MRI to characterize hypoxic tumor subvolumes in comparison to FMISO PET/CT. Consequences for diagnosis and chemoradiation treatment planning in head and neck cancer. *Radiother Oncol*. 2020; 150:128-135.

38. Morand GB, Vital DG, Kudura K, et al. Maximum standardized uptake value (SUVmax) of primary tumor predicts occult neck metastasis in oral cancer. *Sci Rep*. 2018;8:11817.

39. Zhang B, Geng J, Nie F, Li X. Primary tumor standardized uptake value predicts survival in head and neck squamous cell carcinoma. *Oncol Res Treat*. 2015;38:45-48.

40. Minn H, Lapela M, Klemi PJ, et al. Prediction of survival with fluorine-18-fluoro-deoxyglucose and PET in head and neck cancer. *J Nucl Med*. 1997;38:1907-1911.

41. Roh JL, Pae KH, Choi SH, et al. 2-[18F]-Fluoro-2-deoxy-D-glucose positron emission tomography as guidance for primary treatment in patients with advanced-stage resectable squamous cell carcinoma of the larynx and hypopharynx. *Eur J Surg Oncol*. 2007;33: 790-795.

42. Schwartz DL, Rajendran J, Yueh B, et al. FDG-PET prediction of head and neck squamous cell cancer outcomes. *Arch Otolaryngol Head Neck Surg*. 2004;130:1361-1367.

43. Machtay M, Natwa M, Andrel J, et al. Pretreatment FDG-PET standardized uptake value as a prognostic factor for outcome in head and neck cancer. *Head Neck*. 2009;31:195-201.

44. Halfpenny W, Hain SF, Biassoni L, Maisey MN, Sherman JA, McGurk M. FDG-PET. A possible prognostic factor in head and neck cancer. *Br J Cancer*. 2002;86:512-516.

45. Ng SH, Liao CT, Lin CY, et al. Dynamic contrast-enhanced MRI, diffusion-weighted MRI and (18)F-FDG PET/CT for the prediction of survival in oropharyngeal or hypopharyngeal squamous cell carcinoma treated with chemoradiation. *Eur Radiol*. 2016;26:4162-4172.

46. Chawla S, Kim S, Dougherty L, et al. Pretreatment diffusion-weighted and dynamic contrast-enhanced MRI for prediction of local treatment response in squamous cell carcinomas of the head and neck. *AJR Am J Roentgenol*. 2013;200:35-43.

47. Hatakenaka M, Shioyama Y, Nakamura K, et al. Apparent diffusion coefficient calculated with relatively high b-values correlates with local failure of head and neck squamous cell carcinoma treated with radiotherapy. *AJNR Am J Neuroradiol*. 2011;32: 1904-1910.

48. Kato H, Kanematsu M, Tanaka O, et al. Head and neck squamous cell carcinoma: usefulness of diffusion-weighted MR imaging in the prediction of a neoadjuvant therapeutic effect. *Eur Radiol*. 2009;19: 103-109.

49. Kim S, Loevner L, Quon H, et al. Diffusion-weighted magnetic resonance imaging for predicting and detecting early response to chemoradiation therapy of squamous cell carcinomas of the head and neck. *Clin Cancer Res*. 2009;15:986-994.

50. Lombardi M, Cascone T, Guenzi E, et al. Predictive value of pretreatment apparent diffusion coefficient (ADC) in radio-chemotherapy treated head and neck squamous cell carcinoma. *Radiol Med*. 2017;122:345-352.

51. Grueneisen J, Beiderwellen K, Heusch P, et al. Correlation of standardized uptake value and apparent diffusion coefficient in integrated whole-body PET/MRI of primary and recurrent cervical cancer. *PLoS One*. 2014;9:e96751.

52. Wong RJ, Lin DT, Schoder H, et al. Diagnostic and prognostic value of [(18)F]fluorodeoxyglucose positron emission tomography for recurrent head and neck squamous cell carcinoma. *J Clin Oncol*. 2002; 20:4199-4208.

53. Porceddu SV, Pryor DI, Burmeister E, et al. Results of a prospective study of positron emission tomography-directed management of residual nodal abnormalities in node-positive head and neck cancer after definitive radiotherapy with or without systemic therapy. *Head Neck*. 2011;33:1675-1682.

54. Marcus C, Ciarallo A, Tahari AK, et al. Head and neck PET/CT: therapy response interpretation criteria (Hopkins criteria)-interreader reliability, accuracy, and survival outcomes. *J Nucl Med*. 2014;55:1411-1416.

55. Koksel Y, Gencturk M, Spano A, Reynolds M, Roshan S, Cayci Z. Utility of Likert scale (Deauville criteria) in assessment of chemoradiotherapy response of primary oropharyngeal squamous cell cancer site. *Clin Imaging*. 2019;55:89-94.

56. Zhong J, Sundersingh M, Dyker K, et al. Post-treatment FDG PET-CT in head and neck carcinoma: comparative analysis of 4 qualitative interpretative criteria in a large patient cohort. *Sci Rep*. 2020;10: 4086.

57. Kim S, Oh S, Kim JS, et al. Prognostic value of FDG PET/CT during radiotherapy in head and neck cancer patients. *Radiat Oncol J*. 2018; 36:95-102.

58. Helsen N, Van den Wyngaert T, Carp L, Stroobants S. FDG-PET/CT for treatment response assessment in head and neck squamous cell carcinoma: a systematic review and meta-analysis of diagnostic performance. *EJNMMI*. 2018;45:1063-1071.

59. Vainshtein JM, Spector ME, Stenmark MH, et al. Reliability of post-chemoradiotherapy F-18-FDG PET/CT for prediction of locoregional failure in human papillomavirus-associated oropharyngeal cancer. *Oral Oncol*. 2014;50:234-239.

60. Chernock RD, El-Mofty SK, Thorstad WL, Parvin CA, Lewis JS. HPV-related nonkeratinizing squamous cell carcinoma of the oropharynx: utility of microscopic features in predicting patient outcome. *Head Neck Pathol*. 2009;3:186-194.

61. Krupar R, Robold K, Gaag D, et al. Immunologic and metabolic characteristics of HPV-negative and HPV-positive head and neck squamous cell carcinomas are strikingly different. *Virchows Arch*. 2014;465: 299-312.

62. Chan MW, Higgins K, Enepekides D, et al. Radiologic differences between human papillomavirus-related and human papillomavirus-unrelated oropharyngeal carcinoma on diffusion-weighted imaging. *ORL J Otorhinolaryngol Relat Spec*. 2016;78:344-352.

63. Wong KH, Panek R, Welsh L, et al. The predictive value of early assessment after 1 cycle of induction chemotherapy with 18F-FDG PET/CT and diffusion-weighted MRI for response to radical chemoradiotherapy in head and neck squamous cell carcinoma. *J Nucl Med*. 2016;57:1843-1850.